P - 15

N92-24322

Position Determination of a Lander and Rover at Mars With Earth-Based Differential Tracking

R. D. Kahn, W. M. Folkner, and C. D. Edwards
Tracking Systems and Applications Section

A. Vijayaraghavan
Navigation Systems Section

The presence of two or more landed or orbiting spacecraft at a planet provides the opportunity to perform extremely accurate Earth-based navigation by simultaneously acquiring Doppler data and either Same-Beam Interferometry (SBI) or ranging data. Covariance analyses were performed to investigate the accuracy with which lander and rover positions on the surface of Mars can be determined. Simultaneous acquisition of Doppler and ranging data from a lander and rover over two or more days enables determination of all components of their relative position to under 20 m. Acquiring one hour of Doppler and SBI enables three-dimensional lander–rover relative position determination to better than 5 m. Twelve hours of Doppler and either SBI or ranging from a lander and a low-circular or half-synchronous circular Mars orbiter makes possible lander absolute-position determination to tens of meters.

I. Introduction

The planet Mars will undergo an intensive program of unmanned exploration in coming years. In 1993, the Mars Observer spacecraft will begin to map the Martian surface. The Commonwealth of Independent States (former Soviet Union) is scheduled to launch missions to Mars in 1994 and 1996, in which a number of landers and balloons will be deployed. The U.S. Space Exploration Initiative encompasses a broad range of unmanned and manned trips to the Moon and Mars, which will involve a variety of orbiters, landers, and rovers. The presence of multiple spacecraft at Mars could provide the opportunity to perform extremely accurate Earth-based navigation by using a radio metric technique called Same-Beam Interferometry (SBI) [1,2,3,4]. SBI measurements provide information about spacecraft–spacecraft separation in the plane perpendicular to the Earth–spacecraft line of sight, naturally complementing the position and velocity information obtained from Doppler and ranging measurements. SBI could prove to be a valuable navigational tool supporting future Mars missions, potentially aiding in the final hours of Mars approach navigation, enabling improvement of Mars orbiter ephemerides and providing measurements of the relative positions of landers and rovers with an accuracy of several meters.

Radio metric data types currently used by the DSN for performing navigation of interplanetary spacecraft include ranging, Doppler, and delta very long baseline interferometry (ΔVLBI). While the ranging and Doppler systems provide a direct measurement of line-of sight spacecraft range and range-rate, ΔVLBI provides a measure of spacecraft angular position. The current operational DSN ΔVLBI navigation system can provide a measurement of spacecraft angular position, relative to a fixed extragalactic radio source, with an accuracy of about 30 nrad (equivalent to 4 km at a distance of 1 AU). SBI is a variant of ΔVLBI, with a measurement precision of tens of picoradians (equivalent to several meters at a distance of 1 AU). SBI involves observation of two (or more) spacecraft that are so angularly close that they simultaneously lie within the beamwidth of Earth-based antennas. Simultaneous observation of multiple spacecraft enables orders of magnitude of improvement in accuracy because of tremendous error cancellation resulting when spacecraft observables are differenced.

When SBI and Doppler are simultaneously acquired from two landed spacecraft (e.g., a lander and a rover), it is possible to obtain a several-meter-level determination of the relative position of the two spacecraft on the Martian surface. While traversing the Martian landscape, a rover will need to rely heavily on in-situ navigation techniques, possibly including the use of radio links to Mars-orbiting spacecraft. Earth-based Doppler and SBI provide an independent means of establishing the lander–rover relative position at the several-meter level in three dimensions. SBI could serve as a complement to in-situ navigation, or be used to periodically calibrate lander–rover position measurements obtained from local navigation techniques.

Combining SBI and Doppler is not the only means of determining the position of a rover relative to a lander with Earth-based measurements. Simultaneous Doppler and ranging acquired from both spacecraft at one or more DSN antennas also enables accurate determination of spacecraft–spacecraft relative position. A number of Doppler-ranging examples are examined in this study.

Absolute lander position in the Mars reference frame can be established by simultaneously acquiring Doppler and SBI data or Doppler and range data from the lander and a Mars orbiter. The Doppler data are able to determine the lander components in the plane perpendicular to the Mars spin axis; lander–orbiter SBI, or simultaneous Earth-based ranging to the lander and orbiter, constrains the third component of lander position since the orbiter trajectory is tied to the Mars center of mass.

II. SBI Description

SBI provides a measure of spacecraft–spacecraft angular separation as viewed from Earth. Consider two spacecraft at Mars simultaneously transmitting radio signals to two Earth antennas. Because the two spacecraft are very close angularly (the diameter of Mars as viewed from Earth is at most 124 μrad), each Earth antenna can simultaneously acquire the two spacecraft signals (Fig. 1). The signal from a given spacecraft does not arrive at each of the two Earth antennas simultaneously; the delay in signal reception depends on the angle between the vector connecting the two Earth antennas and the vector from the Earth to the spacecraft. However, the measured delay is corrupted by a variety of error sources, including delays caused by system instrumentation and by signal propagation through neutral and charged media. These errors largely cancel when observables obtained simultaneously from two spacecraft are differenced. The resulting double-differenced delay provides an extremely precise measurement of spacecraft–spacecraft angular separation in the direction parallel to the plane-of-sky projection of the Earth baseline.

SBI observables involving two spacecraft and two Earth antennas are obtained by accumulating spacecraft signal phase at each of the two Earth antennas. If the signal transmitted by each spacecraft has frequency f, then the double-differenced delay τ may be expressed as

$$\tau(t) = \frac{(\phi_{12}(t) - \phi_{11}(t)) - (\phi_{22}(t) - \phi_{21}(t)) + b}{f}$$

where $\phi_{ij}(t)$ represents the phase of the signal transmitted from spacecraft i and received at station j, and b is an unknown integer. Because of the unknown integer bias, an SBI measurement does not directly provide the double-differenced delay. However, SBI measurements obtained continuously over a time interval share the same bias and thus provide a precise measure of temporal changes in the double-differenced delay. Given sufficient a priori information about the spacecraft states, the integer cycle ambiguity can be resolved and the absolute double-differenced delay determined. Typically, a priori information about the spacecraft states is not sufficient to determine the integer-cycle ambiguity, and the SBI phase bias must therefore be estimated. If the sigma on the SBI phase-bias estimate is smaller than 1/6 of a cycle of carrier phase, the integer-cycle ambiguity can be resolved with 99-percent confidence.

It is worth observing that there is an alternative scheme for resolving the SBI phase bias in a relatively short track-

ing arc. This strategy requires that the spacecraft transmit a spectrum of several tones, rather than a single carrier. Preliminary SBI group-delay observables are formed from pairs of tones that are spaced by successively wider intervals. For the narrowest tone spacing, the integer phase ambiguity can be resolved from a priori knowledge. If the frequencies of the tone pairs are carefully selected, then once the delay is resolved for a given pair, the accuracy of the resulting delay measurement is sufficient to enable resolution of the integer-cycle ambiguity for the next (more widely spaced) tone pair. One can bootstrap up through a series of increasingly wider spaced tone pairs, until the SBI phase bias for the carrier is resolvable. This technique could enable SBI carrier-phase bias resolution over time scales on the order of minutes.

III. Lander–Rover SBI Error Budget

SBI measurements are corrupted by a variety of sources, including thermal noise in the ground receiver, signal propagation through neutral and charged media, and nonlinearities in the phase response of station instrumentation. The effect of these errors on SBI measurement accuracy is described in the following error budget, which is similar to several previously developed SBI error budgets [1,2,3,4]. Here the SBI error is given in millimeters. The equivalent angular error in spacecraft–spacecraft relative position is obtained by dividing the delay error by the length (in millimeters) of the plane-of-sky projection of the vector connecting the two Earth antennas. If the two Earth antennas are located at the DSN complexes in Goldstone and Canberra, the length of this projection is typically 8000–10,000 km.

The SBI measurement error is computed for three different cases, which are summarized in Table 1. In Case 1, the lander and rover transmit a 2.3-GHz (S-band) signal with omnidirectional antennas. Signal power is 5 W. In Case 2, the spacecraft have 0.5-m diameter directional antennas, and the transmitted signal is 8.4 GHz (X-band), with 10 W of power. Case 3 is identical to Case 2, except that the spacecraft transmit at 32.5 GHz (Ka-band). In all three cases, it is assumed that 34-m DSN antennas are used for reception.

A. System Noise

The system noise error depends on the ratio of received signal power to the noise power generated in the ground receiver. The 1-sec voltage signal-to-noise ratio (SNR_v) has been calculated for each of the three cases listed in Table 1, assuming an Earth–Mars distance of 2.5 AU (the maximum possible), and system noise temperature of 20 K

at 2.3 GHz, 25 K at 8.4 GHz, and 80 K at 32.5 GHz. Antenna efficiency is 0.7. Given these assumptions, SNR_v = 3.6 for Case 1, SNR_v = 152 for Case 2, and SNR_v = 361 for Case 3. The SBI system noise error is given by

$$\varepsilon = \frac{2\lambda}{2\pi SNR_v \sqrt{T}} \text{ mm}$$

where λ is the wavelength of the signal in millimeters, and T is the integration time in seconds. The 2 in the numerator accounts for the fact that a separate error occurs for each of the four received signals. For an integration time of 5 minutes,

$$\varepsilon = 0.664 \text{ mm} \qquad \text{(Case 1)}$$
$$\varepsilon = 0.004 \text{ mm} \qquad \text{(Case 2)}$$
$$\varepsilon = 0.0005 \text{ mm} \qquad \text{(Case 3)}$$

B. Instrumental Phase Dispersion

Uncalibrated phase shifts occurring in station instrumentation produce delays that vary with signal frequency. It should be possible to calibrate these delays to the level of 0.5 deg by using digital circuitry, such as that used in the DSN narrow-channel-bandwidth VLBI System [5]. The SBI error due to instrumental phase dispersion can be computed as

$$\varepsilon = 2 \times \left(\frac{0.5}{360}\right) \times \lambda \text{ mm}$$

where λ is the wavelength of the signal in millimeters, and the factor of 2 accounts for the fact that a separate error occurs for each of the four signal paths. This expression yields

$$\varepsilon = 0.361 \text{ mm} \qquad \text{(Case 1)}$$
$$\varepsilon = 0.100 \text{ mm} \qquad \text{(Case 2)}$$
$$\varepsilon = 0.026 \text{ mm} \qquad \text{(Case 3)}$$

C. Troposphere

The time delay due to signal transit through the tropospheres of Earth and Mars is independent of signal frequency. The SBI error resulting from uncertainty in the zenith delay at the Earth stations is given by

$$\varepsilon = \sqrt{2}\Delta\theta \times 40 \text{ mm} \times \cos(E)/\sin^2(E)$$

where 40 mm is the zenith-troposphere delay uncertainty (after calibration), $\Delta\theta$ (radians) is the difference in lander

and rover elevation as viewed from Earth, and E is the elevation of Mars as viewed from Earth. The factor of $\sqrt{2}$ accounts for an independent error at each Earth station. Assuming an Earth–Mars distance of 2.5 AU, lander–rover separation of 100 km, and elevation of 15 deg, the Earth troposphere delay error is $\varepsilon = 0.0002$ mm.

Water vapor fluctuations in the Earth's troposphere contribute an SBI error of the form [4]:

$$\varepsilon = \sqrt{2} \times 14.4 \times \Delta\theta^{5/6} \text{ mm}$$

For the lander–rover cases considered here, the contribution of water vapor fluctuations to the SBI error is 7×10^{-5} mm.

Viking lander measurements and Viking orbiter radio-occultation measurements of the Mars atmosphere indicate that atmospheric pressure at the Martian surface is less than 10 mb, and that the atmospheric mean molecular weight is 43 [6,7]. To obtain an estimate of the total (un-calibrated) delay through the Mars troposphere, it is assumed that the forces of pressure and gravity on each slice of atmosphere are exactly balanced ($dp/dh = -\rho g$, where p is pressure, h is altitude, ρ is density, and $g \approx 3.7$ m/sec^2 is the acceleration due to gravity at the surface of Mars) and that the atmosphere is an isothermal ideal gas with a constant mixing ratio (which implies that $p/p_0 = \rho/\rho_0$, where p_0 and ρ_0 are the atmospheric surface pressure and density). These assumptions imply a total zenith dry troposphere delay on the order of 40 mm [8]. The Mars troposphere delay error is written as

$$\varepsilon = 0.5\Delta\gamma \times 40 \text{ mm} \times \cos(e)/\sin^2(e)$$

where $\Delta\gamma$ is the difference in Earth station elevation (in radians) as viewed from Mars, and e is the elevation of the Earth as viewed from Mars. The factor of 0.5 accounts for the fact that the Mars troposphere delay error is highly correlated between spacecraft (measurements of the Earth's troposphere indicate density correlations of 90 percent over hundreds of kilometers [9]). For an Earth–Mars distance of 2.5 AU, Earth station separation of 10,000 km, and Earth elevation of 15 deg, the Mars troposphere delay error is $\varepsilon = 0.008$ mm.

Viking lander measurements indicate that columnar water-vapor content in the Mars atmosphere is three orders of magnitude smaller than on Earth; Mars water-vapor fluctuations should not contribute appreciably to the SBI measurement error.

D. Ionosphere

The ionospheres of Earth and Mars introduce interferometric delay measurement errors that are frequency dependent. Measurement of total electron content (TEC) along the line of sight between Earth antennas and Global Positioning System (GPS) satellites can be mapped to the line of sight from Earth antennas to spacecraft at Mars, which provides TEC calibrations at the level of 5×10^{16} electrons/m^2. The SBI error after calibration is expressed as

$$\varepsilon = \sqrt{2}\Delta\theta \times \frac{2233}{\nu^2} \times 5 \text{ mm}$$

Here, the factor of 5 is an upper bound on the derivative of the mapping function, $\Delta\theta$ is the angular separation of the spacecraft as viewed from Earth, and ν is the signal frequency in gigahertz.

Temporal fluctuations in the electron content along the signal through the Earth's ionosphere result in an SBI error of the form [4]:

$$\varepsilon = \sqrt{2}\Delta\theta^{5/6} \times \frac{3510}{\nu^2} \text{ mm}$$

For the three cases under consideration here, the total SBI error due to the Earth ionosphere is:

$\varepsilon = 0.003$ mm   (Case 1)

$\varepsilon = 0.0002$ mm   (Case 2)

$\varepsilon = 0.00001$ mm   (Case 3)

A reasonable estimate of the total zenith Mars ionospheric delay for an S-band signal is 250 mm [6]. The SBI error due to the Mars ionosphere can be written as:

$$\varepsilon = 0.5\Delta\gamma \times \frac{250 \text{ mm}}{(\nu/2.3)^2} \times \cos(e)/\sin^2(e)$$

with e and $\Delta\gamma$ as defined above. Here, a $1/\sin(e)$ ionospheric mapping function is assumed. The factor of 0.5 accounts for correlations between the ionospheric delay on the measurements from each of the spacecraft. The resulting SBI error is:

$\varepsilon = 0.05$ mm   (Case 1)

$\varepsilon = 0.004$ mm   (Case 2)

$\varepsilon = 0.0002$ mm   (Case 3)

SBI errors due to temporal fluctuations in the Mars ionosphere are small, and not considered here.

E. Station Locations and Universal Time/Polar Motion

Uncertainties in Earth station locations and Earth orientation lead to an SBI error of the form, $\varepsilon = \Delta\theta\varepsilon_{SL}$, where ε_{SL} represents the error in relative positions of the Earth stations, and $\Delta\theta$ is the angular separation (in radians) of the two spacecraft as viewed from Earth. The combined station location and Universal Time/Polar Motion (UTPM) uncertainty is taken to be 70 mm, assuming real-time UTPM estimates based on daily GPS measurements combined with VLBI observations [10]. The resulting SBI error is $\varepsilon = 0.00002$ mm.

F. Solar Plasma

An SBI observable is formed by doubly differencing phase measurements made along the four lines of sight connecting two spacecraft and two Earth antennas (Fig. 1). The four signal paths are separated by hundreds or thousands of kilometers while traversing interplanetary space, which results in imperfect cancellation of the delay error induced by charged particles in the solar wind. The solar plasma delay error is inversely proportional to the square of signal frequency and increases as the Sun–Earth–spacecraft angle decreases. A thin-screen frozen turbulence model is used to model the plasma-induced error [11]. For a lander and rover separated by 100 km, and a Sun–Earth–Mars angle of 20 deg, the plasma-induced SBI error is:

$\varepsilon = 0.059$ mm   (Case 1)

$\varepsilon = 0.004$ mm   (Case 2)

$\varepsilon = 0.0003$ mm   (Case 3)

The SBI measurement errors are summarized in Table 2. For Case 1, the measurement error is dominated by system noise, while instrumental phase dispersion is the principal error for Cases 2 and 3. The 0.76-mm measurement error in Case 1 is equivalent to an angular position error of 95 prad, or 14 m in spacecraft–spacecraft separation for spacecraft at a distance of 1 AU (the Earth–Mars distance varies from 0.5–2.5 AU). For Cases 2 and 3, the SBI measurement errors are equivalent to spacecraft–spacecraft separation errors of 2 m and 0.6 m at 1 AU.

IV. Lander–Rover Relative Position Determination

A. Lander–Rover Positioning With SBI and Doppler Data

Covariance analyses were performed to determine the accuracy with which the relative positions of a Mars lander and rover can be determined by using Doppler and SBI data. The lander is located at 0 deg longitude and +30 deg latitude, and the rover is 100 km north of the lander. The Doppler–SBI data-acquisition period ranges from 1–3.75 hr. Analyses were conducted for each of the three radio frequency configurations listed in Table 1.

The simulated data are acquired for August 15, 1994. Lander and rover Doppler data are acquired at Goldstone; SBI data are acquired along the Goldstone–Canberra baseline. All radio links are assumed to be two-way. For Case 1 (2.3-GHz carrier frequency), the 5-min Doppler are weighted at 0.45 mm/sec; for Cases 2 and 3 (8.4-GHz carrier or 32.5-GHz carrier), the 5-min data are weighted at 0.045 mm/sec. The SBI data are weighted in accordance with the error budget presented above.

A summary of the spacecraft estimated and considered (unadjusted) parameters appears in Table 3. Mars UT1–UTC, the orientation of the Mars pole in inertial space, and the ephemerides of Earth and Mars are estimated together with the lander and rover positions. The a priori sigma for Mars pole orientation is 50 μrad in right ascension and declination [12], and the a priori uncertainty of Mars UT1–UTC is a conservative 30 μrad [14]. Considered parameters include Earth and Mars zenith troposphere delays, Earth and Mars zenith TEC, and Earth-station locations. The media sigmas for Earth represent post-calibration uncertainties; those for Mars represent total uncertainties.

As noted above, the SBI-phase observable contains an integer bias that must (initially) be estimated together with the lander and rover positions. If the integer-cycle ambiguity can be resolved, the full strength of the data can be used to estimate the spacecraft positions. Preliminary covariance runs indicated that the integer bias can be unambiguously determined, even for data arcs as brief as 1 hr. For Cases 2 and 3, it was found that fixing the bias in a 3.75-hr data arc marginally improves the lander–rover relative-position uncertainty; for Case 1, results are improved by a factor of 3. For all three cases, fixing the SBI bias in a 1- or 2-hr data arc improves the lander–rover relative-position uncertainty by up to an order of magnitude. All the results appearing in this article were obtained with the SBI bias fixed.

Figures 2–4 present covariance analysis results for a variety of representative cases. In each of these figures, the lander–rover relative-position error is plotted in Mars-centered, Mars-fixed coordinates. The z-direction is parallel to the Mars axis of rotation, the x-direction ("spin radius" direction) points perpendicularly outward from the Mars spin axis through the lander's position, and the

the y-direction (longitude) is perpendicular to the x- and z-directions.

Figure 2 illustrates the relative position accuracy achievable when Doppler data alone are acquired at Goldstone from both the lander and rover. The Doppler signature induced by Mars rotation enables accurate determination of the components of spacecraft separation that lie in the plane perpendicular to the planet's spin axis. However, Doppler data are insensitive to the third component of lander–rover separation; the z-component error is several kilometers.

When SBI and Doppler data are concurrently acquired, all three components of lander–rover separation can be accurately determined; SBI data complement the Doppler data by providing a precise measurement of spacecraft separation in the plane of the sky. Figure 3 shows the relative position accuracy for the lander and rover when 3.75 hr of SBI and Doppler data are acquired. In Cases 2 and 3 (8.4- or 32.5-GHz carrier frequency), the z-component of lander–rover relative separation can be determined to the several-meter level. Note that the SBI data also improve the determination of the x- and y-components. In Case 1 (2.3-GHz carrier), the SBI and Doppler data are somewhat weaker, enabling x- and y-determination at the level of several meters, and z to about 13 m. The lander–rover relative-position errors depicted in Fig. 3 are the root-sum-square (RSS) of the considered and computed errors; in all cases, the computed error is dominant.

If the transmitting and receiving antennas have 10 deg elevation-visibility cutoffs, the maximum length of time that a Mars lander can be observed along the Goldstone–Canberra baseline is about 3.75 hr. However, spacecraft power constraints or antenna-pointing limitations could further restrict the length of time that Mars landers and rovers are able to transmit to the Earth. Figure 4 illustrates relative position accuracy as a function of observation time. In Cases 2 and 3 (8.4- or 32.5-GHz carrier frequency), acquisition of as little as one hour of data enables determination of all three components of lander–rover separation to the few-meter level. In Case 1 (2.3-GHz carrier frequency), a 1-hr data arc does not provide quite the same level of position accuracy, though it does enable RSS lander–rover relative position determination of under 30 m—more than two orders of magnitude improvement over the position accuracy attainable with a 3.75-hr arc of 8.4-GHz (X-band) Doppler alone.

Additional Doppler–SBI cases were investigated with lander–rover separation oriented East–West, and Northeast–Southwest, and with the lander–rover pair located at 0 deg or −30 deg latitude. It was found that

the ability to determine the relative separation of the two spacecraft does not vary significantly with latitude or rover–lander orientation. The uncertainty in the z-component of the rover–lander separation vector changes by between 1 and 3 m as spacecraft latitude and orientation are varied. This variation in z-uncertainty results from slight differences in sensitivity to Mars pole orientation. Because the separation of the lander and rover was relatively small in the cases studied here, sensitivity of the SBI data to Mars pole orientation was not great enough to permit significant improvement upon the a priori uncertainty. However, measurements involving a network of three or more widely spaced Mars landers could enable determination of Mars pole orientation to the meter level.

B. Lander–Rover Positioning With Ranging and Doppler Data

Another method of determining the relative position of two spacecraft on the Martian surface is to simultaneously acquire Doppler and range data from both spacecraft. To determine the relative position accuracy attainable by using this strategy, lander and rover Doppler and ranging passes were scheduled, with the Doppler weighted at 0.045 mm/sec over 5 min, and the ranging data weighted at 1 m. Range measurements were also assigned a 5-m bias to account for uncalibrated delays in the system hardware.

The ability of ranging to resolve the z-component of rover–lander separation depends to some extent on Earth–Mars geometry, which changes significantly over a period of months. Two cases are considered here: (1) data are acquired for August 15, 1994, from the same lander–rover pair considered in the SBI-Doppler example above; and (2) data are acquired for June 2, 1994, from a lander–rover pair with the lander located at 90 deg East longitude, −30 deg South longitude, and the rover 100 km north of the lander. In the first case, Earth declination as viewed from Mars is 3 deg, so Earth–Mars ranging measurements have little projection in the z-direction. In the second case, the declination of Earth is close to 24 deg. In each case, ranging and Doppler data are acquired at the three DSN antennas in Goldstone, Canberra, and Madrid whenever the spacecraft are visible. The estimation strategy is the same as above (Table 3).

Figure 5 illustrates the z-component uncertainty as a function of scan length for the two cases. In the first case (data acquired beginning August 15, 1994), a single day of tracking (the spacecraft are visible from Earth for approximately 11 hr) enables determination of the z-component of lander–rover separation to about 160 m. Dramatic reduction in the z-component error occurs during the second day of tracking; the geometry has evolved

sufficiently so that uncertainties in Mars pole orientation and planetary ephemerides can be separated from relative z-component uncertainties. After three days of data acquisition, the z-component of spacecraft separation is determined to about 15 m. In the second case (data acquired beginning June 2, 1994), acquisition of a single day of Doppler and ranging determines the z-component of rover–lander separation to the 20-m level; multiple-day observations enable modest improvement in the determination of the z-component.

It should be noted that the ability of Doppler and ranging to perform accurate lander–rover relative position determination may be significantly improved if the Mars pole orientation and Mars UT1 are more tightly constrained. Though these parameters are currently known at the 50-μrad level, the monitoring of multiple surface beacons at Mars in the future could enable determination at the level of tenths of microradians.

V. Determination of a Lander's Absolute Position

Simultaneous acquisition of Doppler and SBI data, or Doppler and ranging data, from a Mars lander and orbiter enables accurate determination of the lander's absolute position on the surface of Mars. The Doppler data are able to determine the lander components in the plane perpendicular to the Mars spin axis; lander–orbiter SBI, or simultaneous lander–orbiter ranging, constrains the third component of lander position since the orbiter trajectory is tied to the Mars center of mass.

Two different Mars orbiters are considered in this study—a low circular polar orbiter (LCPO), and a half-synchronous circular orbiter (HSCO). The orbital elements for these spacecraft are listed in Table 4. The reference epoch for each orbiter is August 15, 1994 00:00:00 UTC.

Table 5 lists the estimated and considered parameters and a priori uncertainties for the lander–orbiter covariance analysis. The gravity-field uncertainty is based on an analysis of gravity-calibration orbits for Mars Observer early in its mission.[1] The longitude of the lander is fixed, defining a Mars-centered radio-reference frame. Once the z-height and spin radius of this lander are determined, the locations of other landers or rovers in this frame of reference could be established by performing simultaneous Doppler and SBI or Doppler and ranging measurements, as discussed above.

[1] P. B. Esposito, *Mars Observer Navigation Plan: Preliminary*, JPL D-3820 (internal document), Jet Propulsion Laboratory, Pasadena, California, December 16, 1988.

A. Lander Positioning With SBI and Doppler Data From Lander and Orbiter

In the cases studied here, the SBI data are obtained from the lander and a single orbiter, either LCPO or HSCO. As in the lander–rover analysis presented above, an SBI phase bias was estimated in preliminary runs in order to establish that the integer bias could be unambiguously determined.

The lander–orbiter Doppler and SBI data were scheduled for August 16, 1994 from 10:00 through 23:00 UTC. Doppler data from both spacecraft are acquired continuously at Goldstone during this time; SBI data are acquired when two DSN stations can simultaneously view both spacecraft. Figure 6 portrays the Earth–spacecraft visibility during this period. The lander, located at 100-deg longitude and 0-deg latitude, is visible along the Goldstone–Madrid baseline from 10:50 to 15:05, and is visible along the Goldstone–Canberra baseline from 18:40 to 21:35. The LCPO has a period of approximately 130 min, and is occulted by Mars for about 30 min of each revolution. The HSCO is not occulted by Mars during the period of observation.

Because the angular separation of orbiter and lander as viewed from Earth is larger than in the lander–rover case, the SBI data suffer increased degradation from imperfect cancellation of media effects, particularly the solar plasma. Time-tag synchronization uncertainty between the two stations induces an additional error in SBI measurements involving spacecraft whose range rates have a relative drift over the observation [4]. At present, time tags are known to the 0.1-μsec level. However, nanosecond-level synchronization is feasible and would make this error insignificant. In this study, 8.4-GHz (X-band) lander–orbiter SBI data are weighted at 0.2 mm [3], and 2.3-GHz (S-band) SBI data are weighted at 2.5 mm.

For the lander and the HSCO, Doppler data are weighted as described previously—0.045 mm/sec for 8.4-GHz (X-band) Doppler, 0.45 mm/sec for 2.3-GHz (S-band) Doppler; for the LCPO, Doppler data are *always* weighted at 2.5 mm/sec to reduce sensitivity to uncertainties in the Mars gravity field.

Figure 7 depicts the uncertainties in the lander's z-component and spin radius when Doppler and SBI data are acquired from the lander and orbiter transmitting a 2.3-GHz or 8.4-GHz carrier signal. If the carrier is 2.3-GHz, then simultaneous acquisition of Doppler and SBI from the lander and the LCPO enables determination of the lander's z-component to under 40 m; the error

in the spin radius is about 3 m. If the carrier is 8.4 GHz, the z-component error is below 10 m, while the spin-radius error is at the submeter level. Results of similar quality are obtained when Doppler and SBI are simultaneously acquired from the lander and the HSCO.

B. Lander Positioning With Ranging and Doppler Data From Lander and Orbiter

Simultaneous acquisition of Earth-based ranging and Doppler data also enables very accurate lander-position determination. To study this case, lander and orbiter 8.4-GHz (X-band) Doppler and ranging data were scheduled for August 16 from 10:00 through 23:00 UTC. Data were acquired at a given DSN complex whenever the spacecraft were visible.

Initial covariance analyses indicated that the lander's z-component can be determined to about 130 m if the ranging data have 1-m precision and a 5-m bias. While this level of range data accuracy is representative of the upper limits of the capabilities of the current system, ranging systems with accuracies on the order of tens of centimeters are feasible [15]. For the lander–orbiter cases studied here, the ranging data are assumed to have 30-cm precision, and a 1-m bias due to uncalibrated delays through system hardware.

Figure 8 illustrates the uncertainties in the lander's spin radius and z-height, after 13 hr of 8.4-GHz (X-band) Doppler and precise ranging are simultaneously acquired from the lander and an orbiter. When data are acquired from the lander and either the LCPO or the HSCO, the lander's RSS z-height error is about 30 m. Simultaneous acquisition of Doppler and ranging from the lander and the HSCO enable determination of the lander's spin radius to a few meters. The lander's spin radius can be determined somewhat less accurately if the LCPO is used; the LCPO is more sensitive to gravity mismodeling.

VI. Summary

Radio metric tracking from Earth of multiple spacecraft on the surface of Mars can enable accurate relative and absolute spacecraft-position determination. Simultaneous acquisition of Doppler and ranging enables very accurate relative positioning of Mars landers. Alternatively, SBI combined with Doppler data can enable accurate relative positioning of spacecraft on the surface of Mars with shorter observation times: Few-meter position determination can be obtained with data arcs as brief as 1 hr. Absolute lander-position determination in Mars-centered coordinates is possible by making differential observations of landers and orbiters. The orbiter provides a tie to the Mars center of mass, allowing the absolute lander z-height coordinate to be determined. Range and Doppler or SBI and Doppler can provide 10- to 30-m accuracy for all components of the absolute lander position.

The range and the SBI data types each have advantages that will determine which technique is most appropriate for a given mission scenario. The combination of Doppler and ranging has the advantage of using only one Earth station at a time, but requires ranging transponders on the Mars surface elements and must be acquired in two-way mode. SBI, on the other hand, requires only a simple one-way carrier signal, and thus could be used with very unsophisticated, low-power surface beacons. The inherently high precision of the SBI observable also allows relative rover–lander positions to be determined extremely rapidly from short data arcs. This could have benefits for quickly obtaining daily updates for lander–rover relative separation.

This study has focused on the ability of Earth-based differential tracking to determine positions for surface elements. In the lander–orbiter case, these same differential observations also serve to benefit determination of the orbiter state. Additional analysis must be performed to quantify the benefits of orbiter–lander relative tracking for Earth-based orbiter navigation.

Over the coming decade, a number of opportunities to demonstrate and apply these differential tracking techniques will arise. The SBI technique is currently being tested through a program of observations of the Magellan and Pioneer Venus Orbiter spacecraft at Venus [4]. In the mid-to-latter part of this decade, the United States' Mars Observer and the former Soviet Union's Mars '94 spacecraft will both be at Mars. Relative tracking of these spacecraft, and possibly of landed elements of the Mars '94 mission, will provide a test-bed for differential tracking which could have potential benefits to both missions. Future robotic and manned Mars missions embodied in the Space Exploration Initiative would ultimately benefit from these techniques. As the infrastructure of Mars tracking and navigation resources grows, in-situ tracking techniques will also come into play; nonetheless, Earth-based tracking will continue to play an important complementary role in the overall Mars navigation challenge.

References

[1] J. S. Border and W. M. Folkner, "Differential Spacecraft Tracking by Interferometry," *Proceedings of the CNES International Symposium on Space Dynamics, Nov. 6–10, 1989,* Toulouse, France: Cepadues-Editions, pp. 643–654, 1990.

[2] J. S. Border and R. D. Kahn, "Relative Tracking of Multiple Spacecraft by Interferometry," *Proceedings of the AAS/GSFC International Symposium on Orbital Mechanics and Mission Design,* San Diego, California: Univett, Inc., pp. 441–454, 1989.

[3] W. M. Folkner and J. S. Border, "Orbiter-Orbiter and Orbiter-Lander Tracking Using Same-Beam Interferometry," *Technical Papers, AIAA/AAS Astrodynamics Conference Part 1* (A90-52957 24-13), Washington, D.C.: American Institute of Aeronautics and Astronautics, pp. 355–363, August 20–22, 1990.

[4] J. S. Border, W. M. Folkner, R. D. Kahn, and K. S. Zukor, "Precise Tracking of the Magellan and Pioneer Venus Orbiters by Same-Beam Interferometry," paper AAS 91-191 presented at the AAS/AIAA Spaceflight Mechanics Meeting, Houston, Texas, February 1991.

[5] N. C. Ham, "VLBI System (BLK I) IF-Video Down Conversion Design," *TDA Progress Report 42-79,* vol. July–September, Jet Propulsion Labortory, Pasadena, California, pp. 172–177, November 15, 1984.

[6] G. Lindal, H. B. Hotz, D. N. Sweetnam, Z. Shippony, J. P. Brenkle, G. V. Hartsell, and R. T. Spear, "Viking Radio Occultation Measurements of the Atmosphere and Topography of Mars: Data Acquired During 1 Martian Year of Tracking," *Journal of Geophysical Research,* vol. 84, no. B14, pp. 8443–8456, December 30, 1979.

[7] A. Seiff and D. B. Kirk, "Structure of the Atmosphere of Mars at Mid-Latitudes," *Journal of Geophysical Research,* vol. 82, no. 28, pp. 4364–4378, September 30, 1977.

[8] A. R. Thompson, J. M. Moran, and G. W. Swenson, Jr., *Interferometry and Synthesis in Radio Astronomy,* New York: John Wiley and Sons, 1986.

[9] A. Jursa, ed., *Handbook of Geophysics and the Space Environment,* Air Force Geophysics Laboratory, Springfield, Virginia: National Technical Information Service, 1985.

[10] A. P. Freedman, "Determination of Earth Orientation Using the Global Positioning System," *TDA Progress Report 42-99,* vol. July–September, Jet Propulsion Laboratory, Pasadena, California, November 15, 1989.

[11] R. D. Kahn and J. S. Border, "Precise Interferometric Tracking of Spacecraft at Low Sun-Earth-Probe Angles," paper 88-0572 presented at the AIAA 26th Aerospace Sciences Meeting, Reno, Nevada, January 11–14, 1988.

[12] A. P. Mayo, W. T. Blackshear, R. H. Colson, W. H. Michael, Jr., G. M. Kelly, J. P. Brenkle, and T. A. Komarek, "Lander Locations, Mars Physical Ephemeris, and Solar System Parameters: Determination From Viking Lander Tracking Data," *Journal of Geophysical Research,* vol. 82, no. 28, pp. 4297–4303, September 30, 1977.

[13] A. Konopliv and L. J. Wood, "High-Accuracy Mars Approach Navigation with Radio Metric and Optical Data," paper AIAA-90-2907 presented at the AIAA/AAS Astrodynamics Conference, Portland, Oregon, August 20-22, 1990.

[14] A. Cazenave and G. Balmino, "Meteorological Effects on the Seasonal Variations of the Rotation of Mars," *Geophysical Research Letters*, vol. 8, no. 3, pp. 245–248, March 1981.

[15] L. E. Young, "Improved Ranging Systems," taken from *Relativistic Gravitational Experiments in Space*, NASA Conference Publication 3046, pp. 203–205, NASA, Washington, D.C., June 1988.

288

Table 1. One-second SNR for three different radio frequency configurations.

Carrier frequency, GHz	Case 1 2.3 (S-band)	Case 2 8.4 (X-band)	Case 3 32.5 (Ka-band)
Spacecraft antenna diameter, m	Omni	0.5	0.5
Signal power, W	5	10	10
Ground antenna diameter, m	34	34	34
Earth-Mars distance, AU	2.5	2.5	2.5
Receiver system temperature, K	20	25	80
1-sec SNR_v	3.6	152	361

Table 2. SBI measurement error (in mm) for a Mars lander and rover separated by 100 km. The error is computed for the three different radio frequency configurations listed in Table 1. Integration time is 5 min.

Source of error	Case 1	Case 2	Case 3
System noise	0.664	0.004	<0.001
Phase dispersion	0.361	0.100	0.026
Earth troposphere	<0.001	<0.001	<0.001
Mars troposphere	0.008	0.008	0.008
Earth ionosphere	0.003	<0.001	<0.001
Mars ionosphere	0.050	0.004	<0.001
Station locations/UTPM	<0.001	<0.001	<0.001
Solar plasma (20° Sun-Earth-probe angle)	0.059	0.004	<0.001
Root sum square	0.76	0.10	0.03

Table 3. Estimated and considered parameters for lander-rover covariance analysis.

Estimated parameters	A priori sigma
Lander-Rover relative separation	100 km/component
Right ascension and declination of Mars pole	50 μrad/angle
Mars UT1-UTC	30 μrad
Mars, Earth ephemeris corrections	≈ 1 km/component [13]
SBI phase bias (preliminary runs only)	10^6 km
Range bias (Doppler-ranging runs only)	5 m

Considered parameters	A priori sigma
Mars zenith-troposphere delay uncertainty	40 mm
Earth zenith-troposphere delay uncertainty (after calibration)	40 mm
Mars zenith-TEC uncertainty	5×10^{16} electrons/m^2
Earth zenith-TEC uncertainty (after calibration)	5×10^{16} electrons/m^2
Earth station locations (including UT and polar motion)	70 mm/component

Table 4. Orbital elements for low circular polar orbiter and half-synchronous circular orbiter. Reference epoch is August 15, 1994 00:00:00 UTC.

Spacecraft	Semi-major axis, km	Eccentricity	Inclination, deg	Argument of periapsis, deg	Longitude of ascending node, deg	Mean anomaly, deg
LCPO	4150.0	0.0001	91.0	−90.0	0.0	0.0
HSCO	12868.63	0.0001	55.0	−90.0	0.0	0.0

Table 5. Estimated and considered parameters for lander–orbiter covariance analysis.

Estimated parameters	A priori sigma
Lander spin radius and Z-height	100 km per component
Orbiter epoch state position	10^4 km per component
Orbiter epoch state velocity	10 km/sec per component
Right ascension and declination of Mars pole	50 μrad/angle
Mars, Earth ephemeris corrections	≈ 1 km/component [13]
Mars UT1–UTC	175 μrad
SBI phase bias (preliminary runs only)	10^6 km
Range bias (Doppler–ranging runs only)	1 m

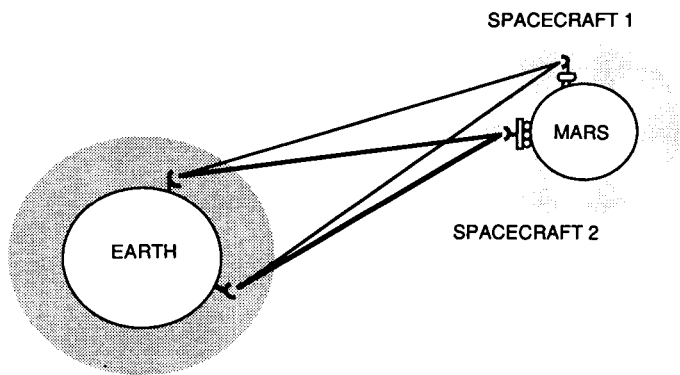| Considered parameters	A priori sigma
Mars and Earth media	(See Table 3)
Earth station locations	70 mm/component
Solar reflection coefficients	10 percent
Atmospheric drag coefficient	20 percent
Bias acceleration	10^{-12} km/sec^2 per component
Mars GM	$3.5 \times 10^{-6} \times$ GM
Mars gravity field	Errors from Mars Observer calibration orbit[2]

[2]Ibid.
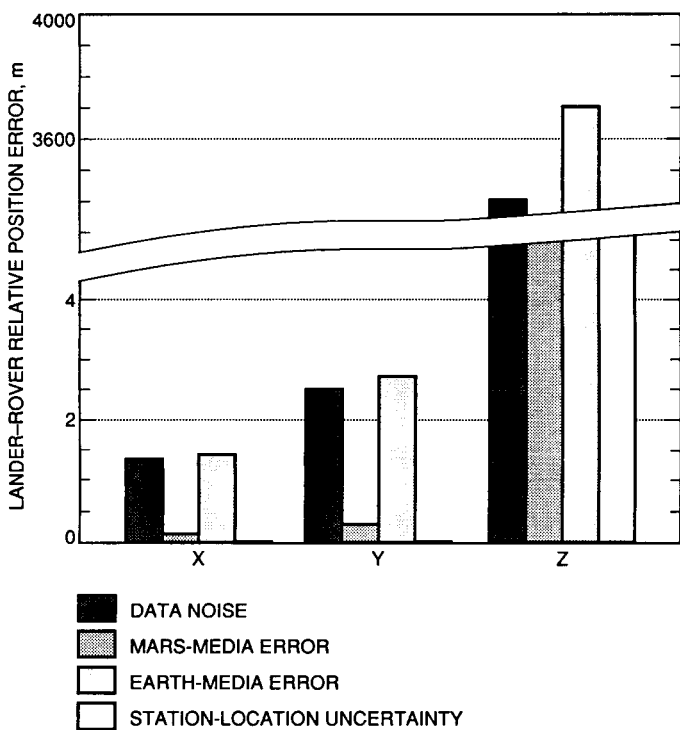
Fig. 1. Same-Beam Interferometry geometry.

Fig. 2. Lander–rover relative position determination using 3.75 hr of Doppler data (carrier frequency 8.4 GHz).
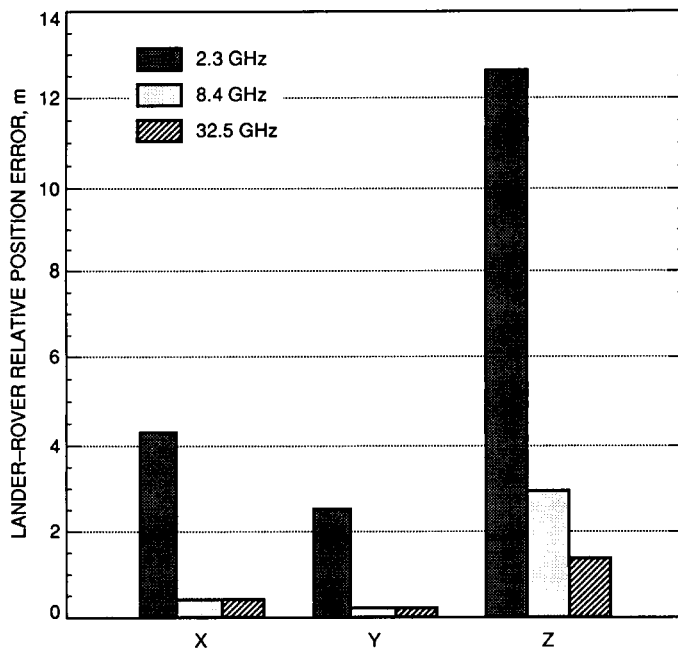

Fig. 3. Lander–rover relative position determination using 3.75 hr of Doppler and Same-Beam Interferometry data. Carrier frequency is 2.3 GHz (S-band), 8.4 GHz (X-band), or 32.5 GHz (Ka-band).
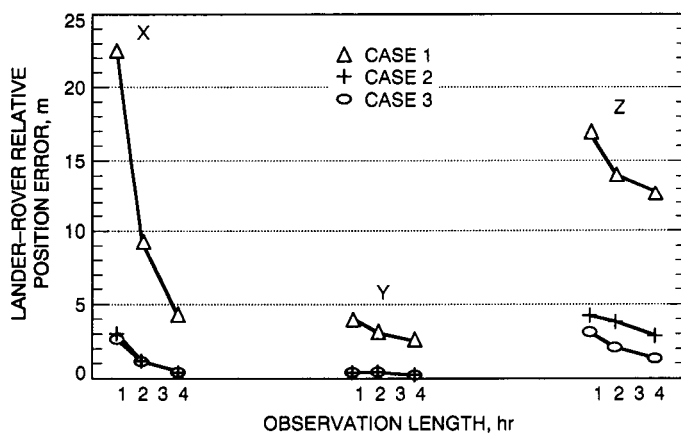

Fig. 4. Doppler and SBI performance as a function of observation length, for each of the cases listed in Table 1. Lander–rover relative position errors are plotted for each component of spacecraft separation after 1 hr, 2 hr, and 3.75 hr.
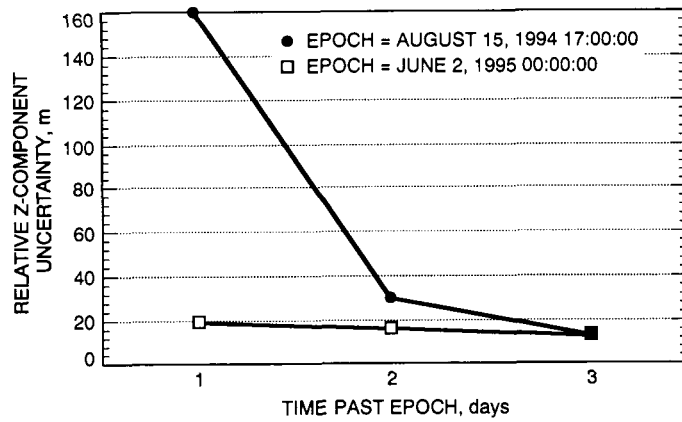
Fig. 5. Uncertainty in z-component of lander–rover relative position when ranging and X-band (8.4-GHz) Doppler are acquired from both spacecraft. On August 15, 1994, the declination of Earth is 3 deg; on June 2, 1995, the declination of Earth is 24 deg.
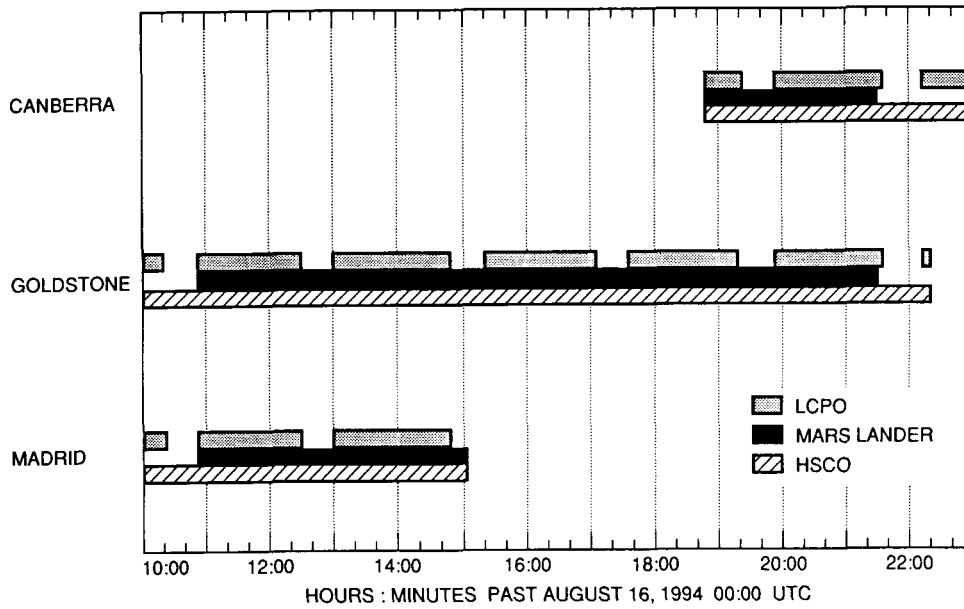

Fig. 6. DSN view periods of low circular polar orbiter, Mars lander, and half-synchronous circular orbiter. The orbital elements are listed in Table 4. The lander is located at 100 deg longitude and 0 deg latitude.

2.3-GHz CARRIER FREQUENCY   **8.4-GHz CARRIER FREQUENCY**

A DATA NOISE
B MARS-MEDIA ERROR
C EARTH-MEDIA ERROR
D STATION-LOCATION UNCERTAINTY

E MISMODELED ORBITER ACCELERATION
F GRAVITY-FIELD UNCERTAINTY
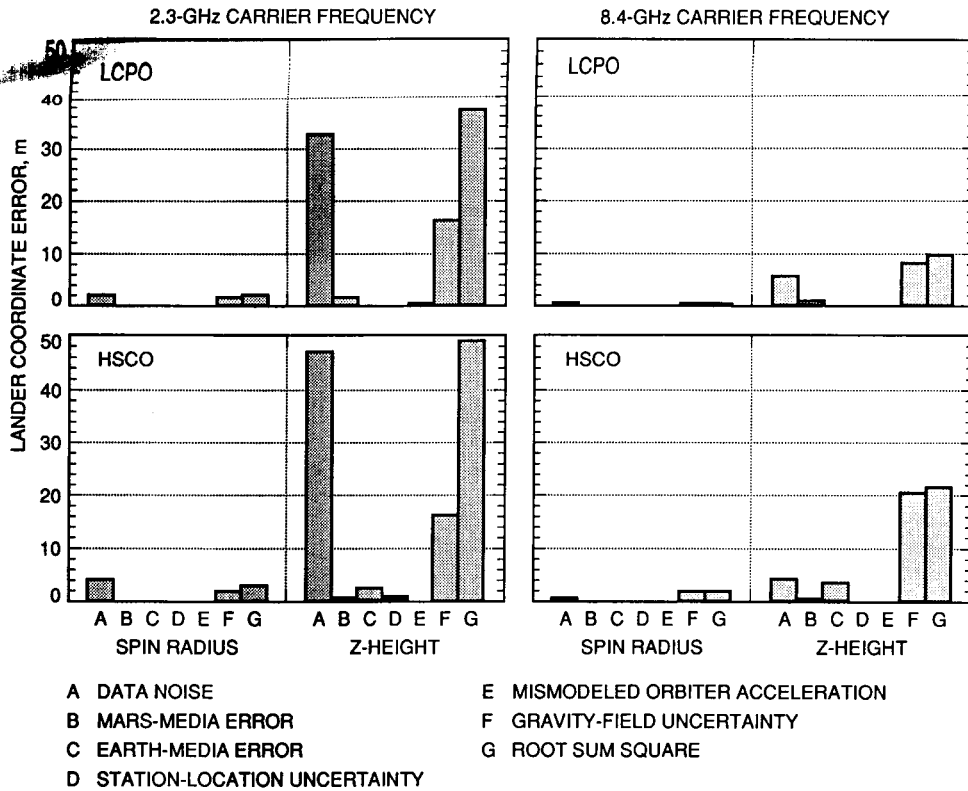G ROOT SUM SQUARE

Fig. 7. Error in lander position when 2.3-GHz (S-band) or 8.4-GHz (X-band) Doppler data and SBI data are acquired from the lander and a low circular polar orbiter or a half-synchronous circular orbiter. SBI data are acquired along both the Goldstone–Canberra and the Goldstone–Madrid baselines.

A DATA NOISE
B MARS-MEDIA ERROR
C EARTH-MEDIA ERROR
D STATION-LOCATION UNCERTAINTY

E MISMODELED ORBITER ACCELERATION
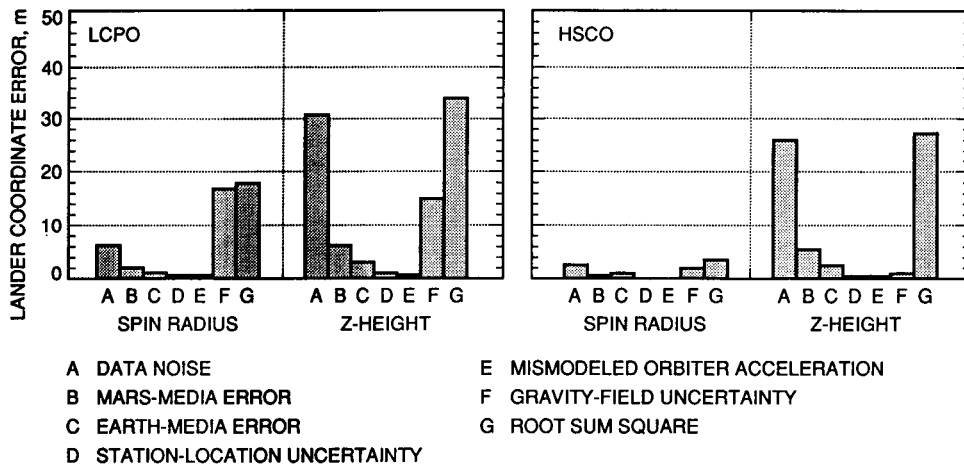F GRAVITY-FIELD UNCERTAINTY
G ROOT SUM SQUARE

Fig. 8. Error in lander position when 8.4-GHz (X-band) Doppler data and 30-cm ranging are acquired from the lander and a low circular polar orbiter or a half-synchronous circular orbiter.